DESIGN AND CHARACTERIZATION OF THREE DIMENSIONAL TWIST-BRAID SCAFFOLDS FOR ANTERIOR CRUCIATE LIGAMENT REPLACEMENT

By

SHREYA MADHAVARAPU

A thesis submitted to the

Graduate School-New Brunswick

and

The Graduate School of Biomedical Sciences

Rutgers, The State University of New Jersey

In partial fulfillment of the requirements

For the degree of

Master of Science

Graduate Program in Biomedical Engineering

Written under the direction of

Dr. Joseph W. Freeman

And approved by

_____

_____

_____

New Brunswick, New Jersey

October 2016

ABSTRACT OF THE THESIS

Design and Characterization of Three Dimensional Twist-Braid Scaffolds for Anterior Cruciate Ligament Replacement

By SHREYA MADHAVARAPU

Thesis Advisor: Dr. Joseph W. Freeman

The anterior cruciate ligament (ACL) is the most commonly injured ligament in the knee, with more than 350,000 ACL injuries reported annually in the United States. Current treatments include the use of autografts and allografts which have a number of disadvantages. Previous attempts to use synthetic materials in ligament replacement have been unsuccessful due to their inability to replicate the long-term mechanical properties of the native ligament. This project focuses on developing twist-braid poly(L-lactic acid) (PLLA) scaffolds for ACL replacement. Poly(ethylene glycol) diacrylate (PEGDA) was incorporated into the twist-braid scaffolds to evaluate its impact on their mechanical behavior. The twist-braid scaffolds were also compared with braided scaffolds. Scaffold mechanical properties were evaluated based on stress-relaxation, tensile and fatigue properties of the braided-only, twist-braid and the twist-braid scaffolds with PEGDA. All the scaffolds exhibited properties comparable to the native human ACL with the twist-braid scaffolds displaying resistance to fatigue. Scaffolds were seeded with rat patellar tendon fibroblasts. The cell viability and amount of protein released was studied over a course of 8 weeks. The scaffolds were stained with picrosirius red after 8 weeks to show

the deposition of extracellular matrix by the cells. The results from this study showed that the twist-braid scaffolds have properties most suitable for ligament replacement.

ACKNOWLEDGEMENTS

I would like to thank my advisor, Dr Joseph W. Freeman for his guidance and aid throughout the course of my project. I would also like to thank my committee members Dr Ronke Olabisi and Dr Michael Dunn for their advice and fellow Musculoskeletal Tissue Regeneration (MoTR) Laboratory members for all their support and help.

I would also like to thank my family and friends for all their encouragement and support throughout this experience.

Table of Contents

List of Figures

List of Tables

CHAPTER 1 - Introduction

1.1 Structure and Function of the Anterior Cruciate Ligament (ACL)

Ligaments can be described as dense connective tissues that connect bones to other bones to form joints. The knee joint is held together by four very important ligaments-the anterior cruciate ligament (ACL), the posterior cruciate ligament (PCL), the medial collateral ligament (MCL) and the lateral collateral ligament (LCL). These ligaments connect the femur and the tibia and play a key role in normal knee kinematics and maintaining joint stability [1,2,3,4,5]. The human ACL is 30-38 mm long and 10-13 mm wide [6]. It consists of 2 major bundles-the posterolateral bundle and the anteromedial bundle [7,8]. These bundles arise on the posteromedial side of the lateral femoral condyle and insert on the anterior part of the tibial plateau [7,9,10]. Between the femoral attachment and the tibial insertion site, the bundles twist 180 degrees [11]. The anteromedial bundle tightens during knee flexion while the posterolateral bundle tightens in extension [9]. This arrangement results in low friction and tension during normal ranges of motion [12].

Ligaments are composed primarily of collagen, which makes up about 75% of the dry weight. Type I collagen accounts for 85% of the total collagen and the rest includes small amounts of types III, V, VI, XI and XIV [2,3,13,14]. Other than collagen, ligaments are also made up of elastin, proteoglycans (<1% of the dry weight), glycoproteins, other proteins, water and cells [2,13,14,15]. Like all ligaments, the ACL displays a hierarchal

structure comprising of collagen molecules, collagen fibrils, fibril bundles and fascicles, which are arranged parallel to the long-axis of the ligament [4,11]. The collagen molecules form fibrils (1-100 nm in diameter) which are then grouped into collagen fibril bundles (1-20 μm in diameter). Multiple fiber bundles form larger bundles known as fascicles (100-400 μm in diameter). The collagen fibrils are responsible for the crimp pattern (periodic change in direction) that is seen with ligaments. In the ACL, this is observed every 45-60 μm [16]. The ligaments are finally enshrouded by a vascularized epiligament sheath [11]. This hierarchical structure is crucial for ligaments to stabilize joints by connecting bone to bone [17].

1.2 Mechanical Behavior of the Anterior Cruciate Ligament

Ligaments exhibit a non-linear stress-strain relationship which can be seen as three different stages. The first stage is the toe region where the ligaments exhibit a low slope i.e. low amount of stress per unit strain. When the ACL is subjected to a force, it is first transferred to the collagen fibrils resulting in their lateral contraction and straightening of the crimp pattern. Once it is straightened, the force is translated as collagen molecular strain [19]. As the force applied increases, the collagen fibrils extend and begin to slide over one another. This happens in the linear region which exhibits a much higher value of slope. In both the toe region and the linear region, the deformation is recoverable. As the amount of force applied increases, the collagen fibrils extend completely and start rupturing, eventually leading to failure of the ACL. This is seen in the yield or failure region.

1.3 Anterior Cruciate Ligament Injury

The knee, which is one of the most complex joints in the human body plays a vital role in locomotion. Knee ligament injuries-sprains and tears most commonly occur in athletes. A few decades ago such injuries would have meant the end of an athlete's career. Today, while most of them are able to return to sport following multiple ligament injuries, they are unable to get back to their previous level of activity [20]. Most ligament injuries are a result of knee twisting, hyperextension, sudden deceleration, sudden change in direction while running or getting hit on the knee [21,22]. These conditions can lead to injury to one or more ligaments. The ACL is the most commonly injured ligament in the knee with over 350,000 injuries reported in the United States every year [23,24]. ACL reconstruction surgery is the standard care procedure which is used to treat such injuries and more than 200,000 such procedures were performed in the US in 2011 [24,26]. ACL injuries require $6 billion annually for acute care alone and the reconstruction procedures increase the health care cost to more than $1 billion [23]. The majority of ACL injuries (~70%) occur while playing sports like soccer, basketball, football and skiing. 30% of these injuries are a result of direct contact while a majority (70%) are caused by non-contact mechanisms [26]. ACL injuries lead to a significant amount of joint dysfunction which over time can cause injury to other tissues in the joint and lead to the development of degenerative joint diseases like osteoarthritis and osteoporosis [22]. The ACL is completely surrounded by synovial fluid and lacks vascularity which is the main reason why it is unable to heal completely following an injury [17]. Hence, an ACL reconstruction is performed which requires an ACL graft.

1.4 Current Treatment Strategies

ACL reconstruction or ACL replacement surgery is the widely preferred treatment option for ACL injuries. This is due to a higher rate of satisfaction and a lower degree of osteoarthritis that are associated with it [23]. Traditionally, biological grafts have been used to treat ACL injuries [19]. These include the autografts, allografts and the xenografts [18]. The gold standard for ACL reconstruction surgery is a bone-tendon-bone graft [1]. Long-term evaluation has shown that biological grafts have a 85-90% success rate in terms of patient satisfaction and restoration of knee stability [23,27]. While these grafts offer good initial mechanical strength, promote cell proliferation and the growth of new tissue, they suffer from a large number of disadvantages and most patients do not return to pre-injury level of activity [19]. Despite all these drawbacks, a bone-tendon-bone graft remains the gold standard for ACL injury treatment.

1.4.1 Autografts

In a majority of cases, the patient's own patellar tendon, hamstring tendon or the quadriceps muscle are harvested [28,29]. This is the safest and fastest-healing source of tissue for ACL reconstruction. Autografts significantly promote bone-to-bone healing, fixation securing and return to pre-injury level of activity [23]. While these are the safest options, they require two surgeries-one to harvest the tissue and the other for ACL reconstruction [19]. This contributes to increased pain, donor site morbidity and a longer healing time [18,29,30,31]. Other complications associated with autografts include

anterior knee pain, kneeling pain, patellar fracture, nerve injury, graft failure, patellofemoral pain, decreased range-of-motion, and muscle atrophy [23,27,31,32].

1.4.2 Allografts

Allografts are tissues obtained from donors. These are usually the patellar ligament or the Achilles tendon [4,28,33]. Unlike autografts, patients undergoing ACL reconstruction with allografts only undergo one surgery reducing the total time for the surgery. With allografts, there is a lower incidence of postoperative arthrofibrosis and knee stiffness [23,34]. These have a better short term function when compared to autografts. Despite the advantages, there are a number of complications associated with these grafts. The most important ones are the risk of disease transmission, infection and possible immune rejection [29,32,35]. A number of sterilization techniques are applied to overcome the risk of disease transmission and infection but these lead to inferior mechanical properties in terms of knee laxity, stress to failure, postoperative traumatic rupture rate [23,30]. There is also delayed incorporation, bone tunnel enlargement and slower remodeling activity when compared to autografts due to lower cellularity and the absence of revascularization [23]. Another important concern regarding allografts is the limited supply of donors which is unable to meet the escalating demand for allograft tissue [18,27].

1.4.3 Xenografts

These are tissues that are obtained from a different species. For ACL reconstruction porcine grafts have been used. Xenografts are scarcely used and are not the most preferred biological grafts due to a number of associated disadvantages. These include the risk of infection, disease transmission and immunological rejection [23]. Similar to allografts, these also undergo various stages of sterilization to overcome the risks of infection but this again leads to reduced mechanical stability of the grafts.

1.4.4 Synthetic Grafts

Over the last few decades, various synthetic grafts have made their way into the commercial space. Synthetic grafts have a lot of advantages over biological grafts. They offer a simple and easily reproducible option. With these grafts, there is no need to worry about donor-site morbidity, risk of infection or disease transmission. They require a shorter surgery, show significant strength and are associated with an accelerated rehabilitation period [30]. Synthetic grafts can either be prosthetics or augmentation devices. While these grafts gained some popularity in the 1970s and the 1980s, it was under very limited conditions [1,30,36]. Most of these grafts failed due to their inability to mimic the mechanical properties of the human ACL. The Gore-Tex (braided polytetrafluoroethylene fibers) and the Stryker-Dacron ligament (woven polyethylene terephthalate) were approved by the FDA for use as ligament prosthesis. The Leeds-Keio prosthesis was another such device which was popular outside the United States [30]. Results from ACL reconstructions using these prosthesis showed foreign-body reactions

and inflammations, limited integration between the graft and the host tissue, material degradation, poor abrasion resistance and fatigue failure [15,19,23,32,36,37]. These ligament prosthesis were withdrawn from the market due to their long-term drawbacks which included premature graft failure, synovitis, osteoporosis and osteoarthritis [1,19,23,27,30,36,37,38]. Augmentation devices such as the Kennedy Ligament Augmentation Device (LAD) were designed to promote integration of the graft and the host. But these were also fraught with complications such as inflammatory reactions and graft failure [27].

1.4.5 Tissue Engineered Grafts for ACL Reconstruction

The limitations associated with the current grafts-both biological and synthetic, have resulted in looking towards tissue engineering for alternate options. Tissue engineering has been described as a multidisciplinary field that incorporates the principles of biochemistry, engineering and material science to develop substitutes for replacing injured or diseased tissues [4,27,39,40]. Tissue engineering can be used to make polymer scaffolds that mimic the mechanical properties of the native ACL, promote cell adhesion, proliferation and differentiation and eventually degrade away to be replaced by native tissue at the site of implantation. A tissue engineered ligament would require a structural scaffold that facilitates cell adaptation, cells that have the capacity to proliferate and synthesize matrix and an environment that provides sufficient nutrient transport and appropriate regulatory stimuli. An ideal graft for ligament regeneration would be a three dimensional porous scaffold/structure built from biocompatible and biodegradable

materials (with a controlled degradation profile) [18,43]. Such a scaffold has to promote cell growth while delivering factors required for the growth and differentiation of the cells. Since the rate at which a ligament heals is very slow, such a graft would also have to maintain its mechanical properties while undergoing degradation and allowing the formation of neotissue [19,23]. While their have been numerous attempts so far, none have been able to mimic all of the characteristics of a native human ACL in terms of mechanical strength, elasticity, compliance and durability while at the same time being biocompatible and having no adverse side-effects.

1.5 Aim of the Project

This project aims to combine the techniques of fiber twisting and 3D braiding to fabricate three dimensional twist-braid scaffolds that mimic the hierarchal structure and mechanical properties of a human ACL. These scaffolds were mechanically characterized based on their tensile, viscoelastic and fatigue properties. The cell biocompatibility was studied based on cell viability and protein.

CHAPTER 2 - Scaffold Fabrication and Characterization of Scaffold Structure, Mechanical Properties and Cell Biocompatibility

This project involved the fabrication of two types of scaffolds-the braided only and the twist-braid scaffolds. A hydrogel phase was incorporated into the fibrous scaffolds in order to increase the viscoelastic behavior of the scaffold and act as a carrier for tenogenic factors in future studies. Scaffold structure was characterized by determining the cross-sectional area, weight, pore size and distribution. Stress-relaxation and tensile tests were conducted to analyze the scaffold mechanical properties. Fatigue analysis was performed by subjecting the scaffolds to cyclic strain. The scaffolds were seeded with cells, cell viability and the amount of protein released was determined and the scaffolds were stained for collagen deposition.

2.1 Materials and Methods

The Poly (L-lactic acid) (PLLA) fibers (120 denier/30 microfilaments (60 gm)) used to fabricate the different types of scaffolds were purchased from Biomedical Structures, RI. Two types of scaffolds were made-the twist-braid scaffolds and the braided-only scaffolds. Each of these scaffolds are composed of 288 PLLA fibers.

2.1.1 Fabrication of Twist-Braid (TB) Scaffolds

First, fiber yarns were made using a previously developed method [19]. Briefly, Four fibers, each of length 32 cm were cut and bundled together to form a fiber bundle. Three such fiber bundles were wound onto the posts of a Conair device (Model QB3ECS, Conair Corporation, East Windsor, NJ) such that only 16 cm of each bundle was available for twisting. Each bundle was first twisted onto itself for 5 seconds followed by twisting the three bundles onto one another for 3 seconds in an anti-clockwise direction to form a two dimensional yarn. Once the first 16 cm was twisted, the remaining bundle was unwound, the length was adjusted to 16 cm and the same steps were repeated for twisting. The length and twisting times were chosen based on the methods previously developed by Freeman et al. [19]. Twenty-four such yarns were used to make the 3D twist-braid scaffolds. Fishing line was attached to the two ends of the yarns using epoxy and was wound on the bobbins placed on the braiding machine carriers. The 24 yarns were braided using the MoTR Lab's Custom 3D Braiding Machine at a height of 31 cm to get a braiding angle of 72°. This angle was chosen based on previous experiments done in the lab which showed that braids with this angle have tensile properties most comparable to the native human ACL.

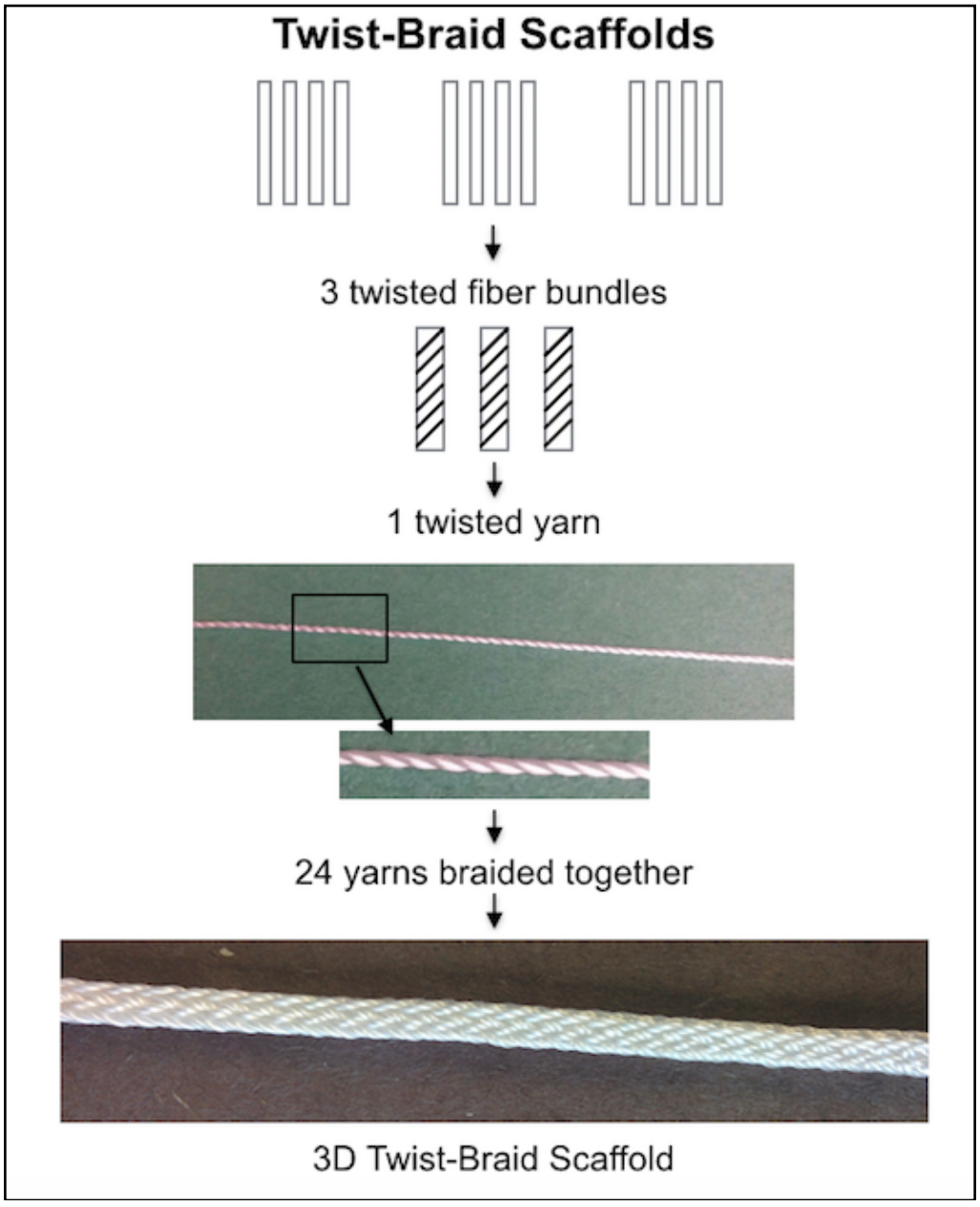

Figure 1: Flowchart showing the steps involved in the fabrication of 3D Twist-Braid Scaffolds

2.1.2 Fabrication of Braided-Only (BO) Scaffolds

12 fibers were cut and bundled together. Twenty-four such bundles were attached to the Braiding machine and braided together to form the Braided-Only scaffolds.

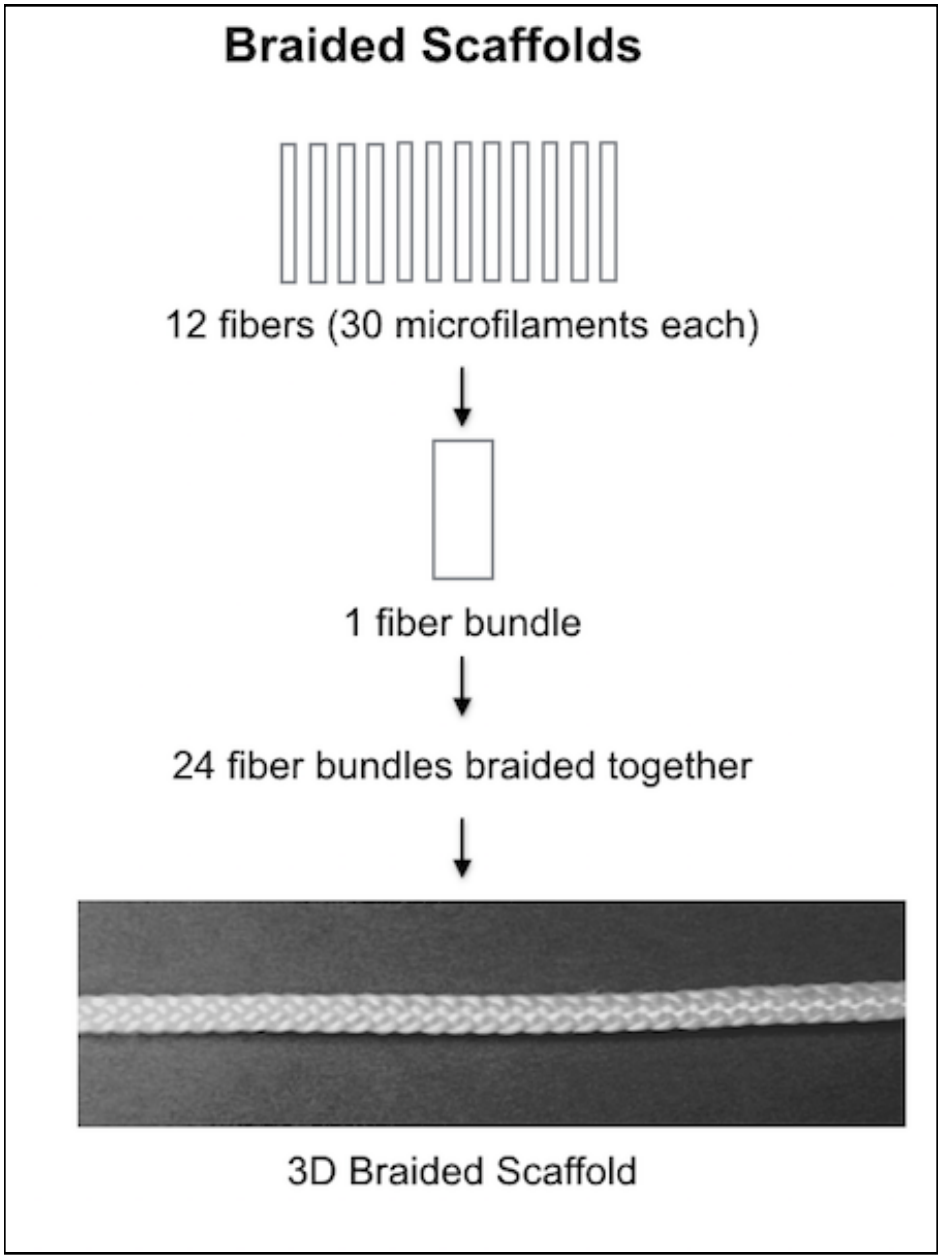

Figure 2: Flowchart showing the steps involved in the fabrication of 3D Braided Scaffolds

2.1.3 Incorporation of Hydrogel

Poly (ethylene glycol) diacrylate (PEGDA, molecular weight 4000 Da, Monomer-Polymer and Dajac Labs, Trevose, PA) was incorporated into the Twist-Braid Scaffolds. The PEGDA was first dissolved in deionized water to make a 10% w/v solution. A 1% (w/v) solution of photoinitiator comprising of 2,2-dimethoxy-2-phenyl acetophenone, n-vinyl-2-pyrrolidinone (300 mg/mL) was added to it. This was then incorporated into the TB scaffolds in two different ways.

- **Hydrogel Scaffolds (HS)**: The TB scaffolds, after braiding were vacuum soaked in the hydrogel for 5 minutes, attached to a rotating device and rotated under UV light (365 nm) for 1 minute.
- **Hydrogel Yarns (HY)**: The yarns, prior to braiding were vacuum soaked in the hydrogel for 5 minutes. Each yarn was then exposed to UV light for 30 seconds on each side and allowed to dry overnight. The yarns with the hydrogel were then braided to obtain the 3D scaffold.

2.1.4 Pore size and distribution

Scaffold pore size was determined using the LEP-1100A Liquid Extrusion Porosimeter (PMI, Ithaca, NY). Scaffolds, approximately 1 cm in length were first vacuum soaked in wetting fluid (Galwick, surface tension 15.9 dynes/cm, PMI, Ithaca, NY) for 30 minutes. These were left to soak in Galwick overnight. A non-porous plastic sheet was cut to obtain circular pieces of diameter 2 cm. A small rectangular section was cut in the center of this circular piece of plastic and the scaffold to be tested was glued over it. It was

ensured that the entire rectangular portion was completely covered by the scaffold, leaving no gaps. The scaffold, now on the circular piece of plastic, was placed in the testing chamber and the sample chamber was placed over it. The chamber was filled with Galwick and the scaffold was allowed to soak in it for 7 to 10 minutes. The piston was then moved down and the test was started. The median pore size and pore size distributions were obtained for the braided-only and the twist-braid scaffolds (n=3).

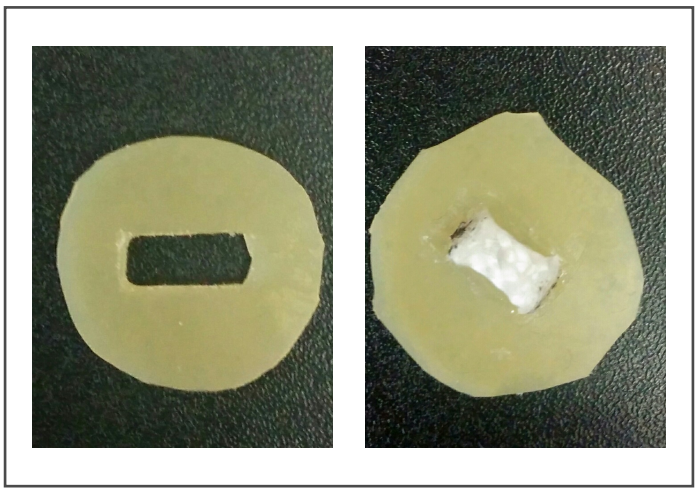

Figure 3: (a) Non-porous plastic base, (b) Scaffold placed over the opening.

2.1.5 Mechanical Characterization

The Instron (Model 5869, Norwood, MA) and MTS (Tytron 250, Eden Prairie, MN) mechanical testing systems were used to determine the scaffold mechanical properties. Scaffold samples of length 3.5 cm were used for the tests. The ends of each scaffold were coated with a castable epoxy (Smooth-on, Inc. Macungie, PA) to prevent them from slipping out of the grips during a test. A gauge length of 15 mm and n=5 was chosen for

all the tests. All the scaffolds were vacuum soaked in phosphate buffered saline (PBS) for 30 minutes prior to testing. During the tests, PBS was sprayed on the scaffolds to keep them moist.

Stress relaxation tests were performed using the Instron to determine the scaffold viscoelastic properties. The scaffolds were loaded to 50 N at 0.3 mm/sec and then allowed to relax for 1800 seconds. The normalized stresses at intervals of 200 seconds were calculated for all the groups i.e. the BO, TB, HS and HY scaffolds.

To test for tensile properties, the instron with a 500 kN load cell was used. The scaffolds were first preloaded to 0.2 N and then extended to failure at a strain rate of 0.4 mm/sec (2%/s) [25]. The ultimate tensile strength (UTS), elastic modulus of the linear region, the length of the toe-region and the strain at failure were obtained from the stress-strain data.

Scaffolds were subjected to cyclic strain using the MTS Tyron 250 in order to study their creep properties. They were first extended to 10% their gauge length i.e. to 16.5 mm. The 10% was chosen based on the data that was obtained from the tensile tests, which showed that the toe region of the scaffolds is about 8 to 10%. Following this, cyclic strain of 2% i.e. 0.3 mm was applied at a frequency of 1 Hz for 2000 cycles. The samples were then stretched out to failure at 0.4 mm/sec using the Instron. The resultant tensile properties i.e. the maximum load, UTS, strain at failure and modulus were compared to those obtained from the tensile tests conducted prior to fatigue.

2.1.6 Sterilization of Scaffolds

The four different types of scaffolds (BO, TB, HS, HY and n=6 for each), each of length 9 mm were first vacuum soaked in 70% ethanol for 30 minutes. This was done to allow the ethanol to penetrate into the scaffolds and reduce the risk of possible contamination. The scaffolds were then placed in separate wells in a 48 well plate and sterilized by exposing each side to UV light for 30 minutes.

2.1.7 Cell Seeding

Rat patellar tendon (rPT) fibroblasts were used for the cell studies. These cells had been previously isolated in the lab using the explant+outgrowth method from the patellar tendons of a skeletally mature male Sprague Dawley rat. Cryopreserved cells were thawed and expanded in α-MEM (Gibco® by Life Technologies, Carlsbad, CA) supplemented with 10% fetal bovine serum (FBS) and 1% penicillin and streptomycin (P/S) (Gibco® by Life Technologies, Carlsbad, CA). The cells were grown to about 80% confluence in the growth medium at 37 °C and 5% CO_2. The scaffolds, after sterilization were soaked in media (α-MEM, 10% FBS, 1% P/S) overnight. This was done so as to promote cell adhesion to the scaffolds when cells were seeded the next morning. They were seeded at a density of 100,000 cells/scaffold. Cells were also seeded on the TCP to serve as an additional control. The cell seeding efficiency was calculated at day 1 by counting the number of cells that were attached to the well plate. Media was changed 3 times a week.

2.1.8 Cell Viability - PrestoBlue Assay

PrestoBlue® reagent (Invitrogen, Frederick, MD) contains a blue colored compound that is cell-permeant. When combined with media, it is rapidly taken up by cells. Viable cells present a reducing environment which changes the blue to an intensely red-fluorescent dye, which can be detected by measuring fluorescence or absorbance. The PrestoBlue assay measures mitochondrial activity which is being used an indirect measure of cell viability. PrestoBlue assay (n=6) was run on Day 1 after transferring the scaffolds into a new 48 well plate. The PrestoBlue solution was prepared (in the dark) using media and the PrestoBlue® reagent in the ratio of 10:1. Media was removed and the cells were washed with PBS. The PrestoBlue solution was then added to each well (again in the dark), the well plate was covered with aluminum foil and placed in the incubator for 1 hour. Following incubation, triplicates of each sample were taken and added to a 96 well plate. This plate was covered with the foil until it had to be read using the plate reader. PrestoBlue assay was also run on Days 3, 7, 14, 21, 28 and then at 6 weeks and 8 weeks

2.1.9 Total Protein Estimation - BCA Assay

The amount of total protein that was released into the media was estimated at Days 1, 3, 7, 14, 21, 28, 6 weeks and 8 weeks (n=6). For this assay, media was collected at every time point that it had to be changed i.e. 3 times a week. A 10x dilution of samples for each time point was used. The standards for the assay were prepared according to the Pierce BCA Protein Assay protocol. 25 µl of the standards and samples (duplicates) were pipetted into a 96 well plate. 200 µl of the BCA working reagent was then added to each

well. After incubating for 30 minutes, the plate was placed in a plate reader and the values of absorbance were noted. A standard curve was plotted using the values obtained for the standards. The values of the samples were then compared to the standard curve to get the amount of total protein present in each of the samples. The total protein concentration obtained for the media was subtracted from the concentration obtained for each individual sample to normalize the results.

2.1.10 Picrosirius Red Staining and Quantification

The scaffold samples, after 8 weeks were stained for collagen using the Picrosirius Red Stain Kit (Polyscience, Inc., Warrington, PA). The images were taken using a Nexus 5 8MP camera and analyzed with ImageJ. After converting them to 8-bit grayscale images, the mean intensity of the pixels was calculated and compared.

2.1.11 Scanning Electron Microscopy

After the 8 week cell study, the cells were fixed on the scaffolds. The scaffolds were frozen and then lyophilized. The dry scaffolds were sputter coated and then imaged to show the deposition of extracellular matrix.

2.1.12 Statistical Analysis of Data

All results were expressed as mean ± standard deviation. Differences between the groups were analyzed using one way ANOVA with Fisher's LSD, with $p<0.05$ considered to be significant.

2.2 Results

2.2.1 Cross-sectional Area and Weight of Scaffolds

The TB scaffolds displayed a significantly larger cross-sectional area (8.23 ± 0.29 mm^2) than the BO scaffolds (6.84 ± 0.32 mm^2). The two scaffolds with the hydrogel also exhibited significantly greater cross-sectional areas (HS 8.75 ± 0.62 mm^2 and HY 9.56 ± 0.35 mm^2) when compared to the TB and the BO scaffolds. The cross-sectional area of the HY scaffolds was also significantly higher than that of the HS scaffolds.

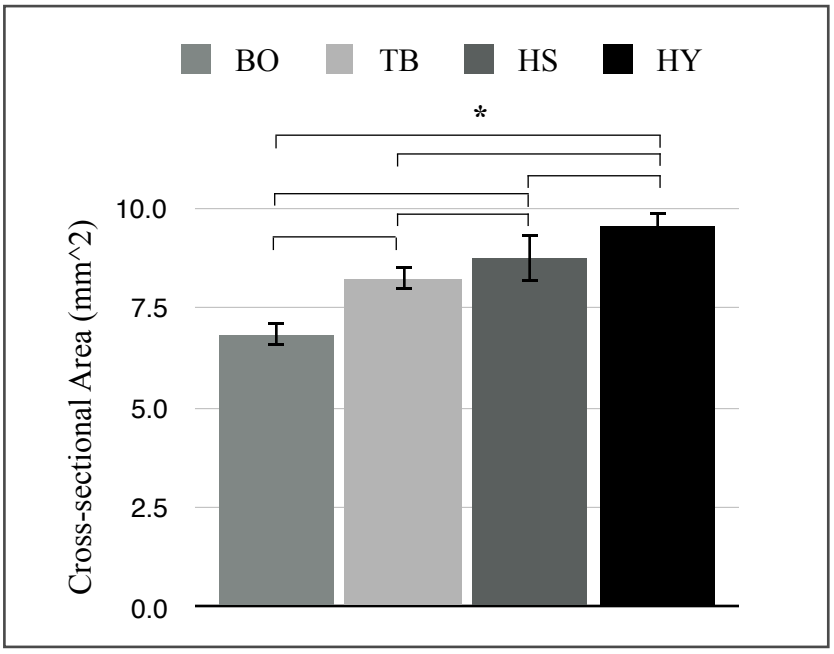

Figure 4: Cross-sectional areas of four scaffolds. The * denotes that the difference is statistically significant ($p<0.05$)

The TB, BO, HS and HY samples were weighed to determine the weight per unit length (i.e., 1 cm). The TB scaffolds (50.18 ± 2.97 mg), HS scaffolds (52.39 ± 1.89 mg) and the HY scaffolds (57.78 ± 4.37 mg) all weighed significantly more than the BO scaffolds (47.83 ± 2.17 mg). The weight of the HY scaffolds was also significantly greater than that of the TB and the HS scaffolds.

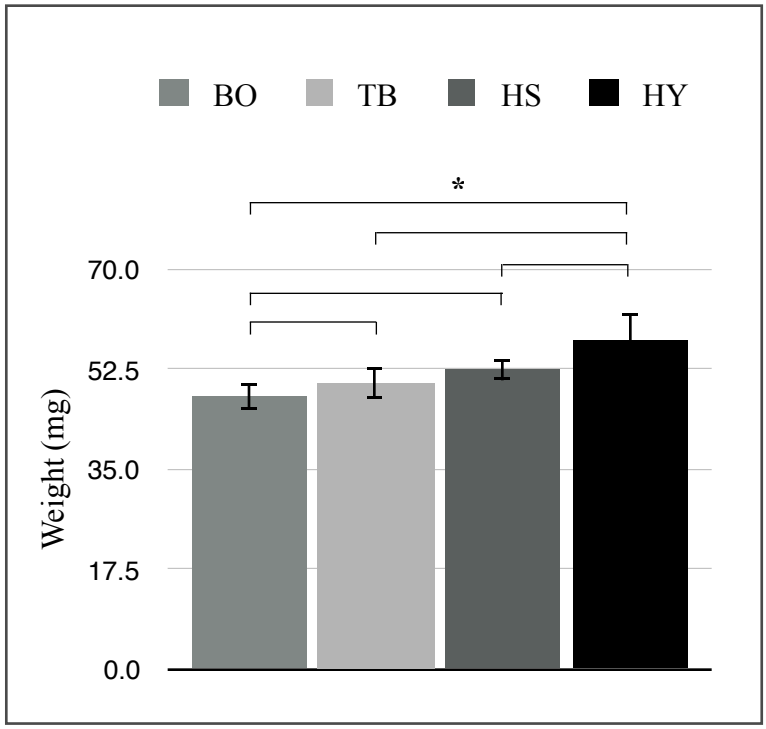

Figure 5: Chart showing the weight per unit length (1 cm) of the scaffolds. A * indicates a significant difference ($p<0.05$)

2.2.2 Pore Size and Distribution

The BO scaffolds displayed a median pore diameter of 73.51 ± 10.58 μm. The median pore diameter of the TB scaffolds was significantly lower at 39.04 ± 7.78 μm.

The median pore diameter indicates that 50% of the pores have pore diameters smaller than this value and the other 50% have larger diameters. For the BO scaffolds, it was observed that approximately 50% of pores were in the range of 70 to 100 μm. For the TB scaffolds more than 80% of the pore sizes were below 70 μm.

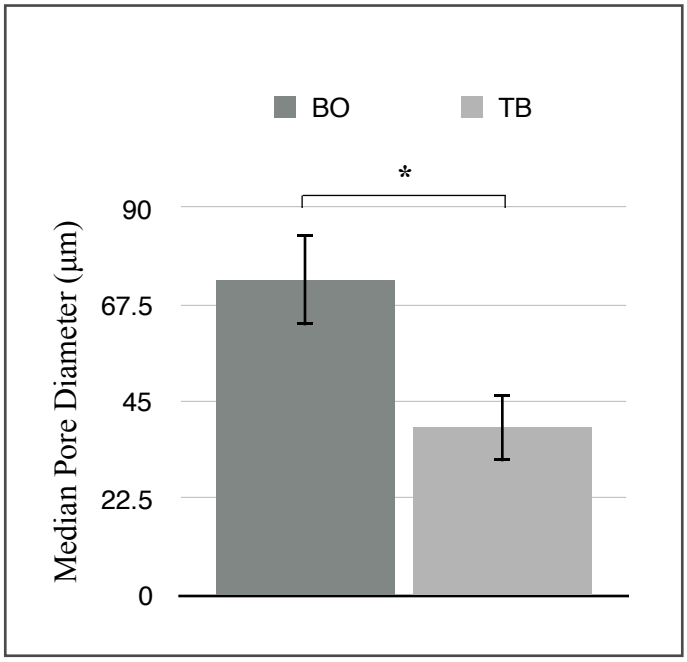

Figure 6: Median pore diameter of BO and TB scaffolds

2.2.3 Viscoelastic Properties

The differences between the TB, HS and HY were statistically insignificant at all the time points. The BO scaffolds, when compared to the other three displayed significantly higher normalized stresses at all the time points. Normalized stresses for the twist-braid scaffolds (with and without hydrogel) at 1000 seconds ranged from 61.3 ± 4.8% for the HS, 64.7 ± 3.3% for the HY to 64.9 ± 2.8% for the TB scaffolds. The normalized stress for BO scaffolds was significantly higher at 70.5 ± 2.1%.

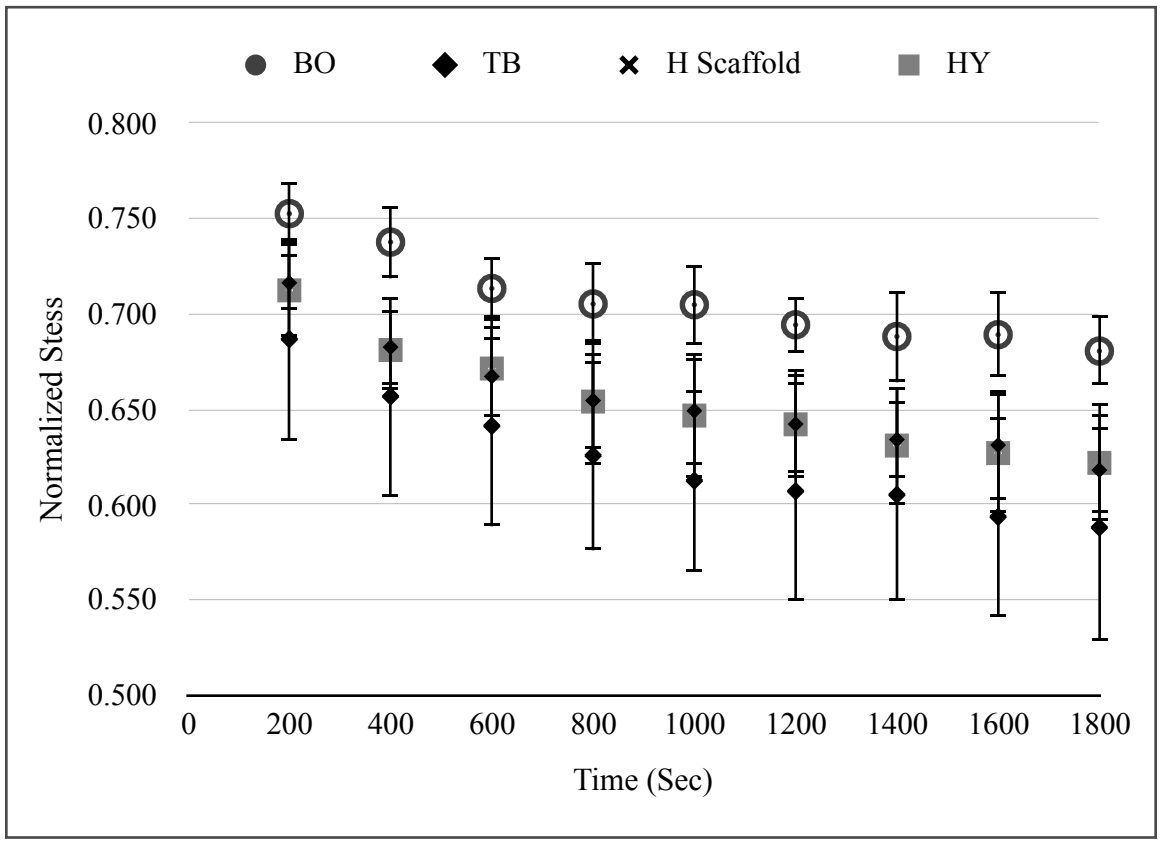

Figure 7: Stress relaxation data obtained for all the scaffolds after a load of 50 N (n=5)

2.2.4 Tensile Properties

The following figure (Figure 8) shows the stress-strain graphs obtained for the BO, TB, HS and HY scaffolds.

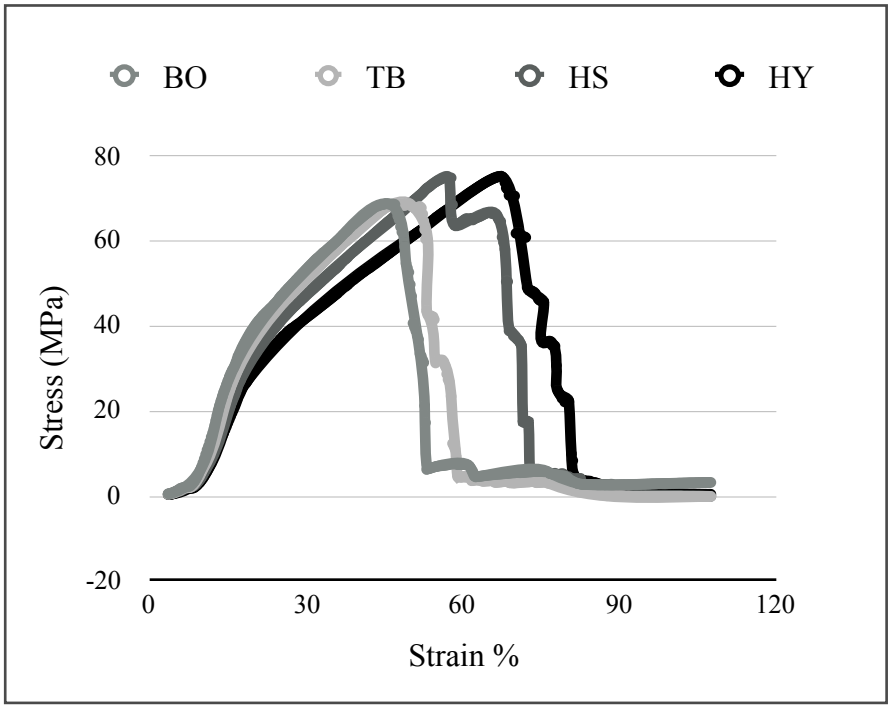

Figure 8: Stress-Strain data obtained for the different scaffolds

The BO and TB scaffolds were able to withstand maximum tensile loads of 614.76 ± 27.17 N and 593.35 ± 18.28 N respectively. The HS (691.34 ± 27.19 N) and HY (734.42 ± 30.18 N) scaffolds displayed significantly higher maximum loads than both the BO and TB scaffolds. The BO scaffolds (86.38 ± 5.46 MPa) exhibited the highest ultimate tensile strength (UTS). The UTS for the TB (70.83 ± 3.40 MPa) and HY (77.41 ± 4.37 MPa) were significantly lower than that of the BO scaffolds. The TB scaffolds showed a significantly lower UTS than the HS (81.59 ± 5.96 MPa) and the HY scaffolds.

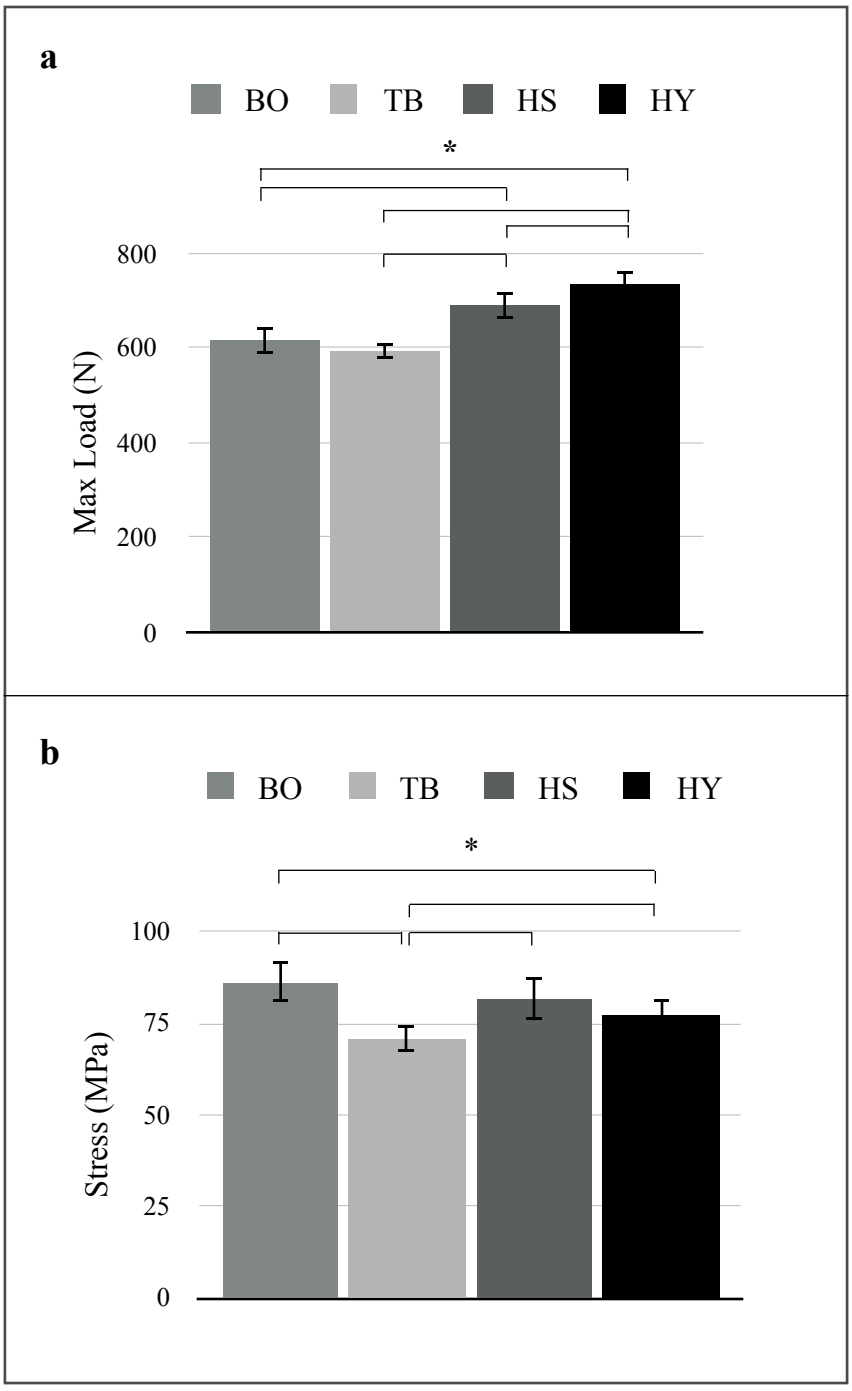

Figure 9: (a) Maximum tensile load (b) Ultimate tensile strength (UTS)

The end of the toe region was noted as the point where the slope increased by 200%. The scaffolds showed toe regions ranging from about 8 to 10%. The BO and HS scaffolds displayed toe region of 8.42 ± 0.75% and 8.53 ± 1.66%. The HY scaffolds displayed a significantly larger toe region (9.74 ± 1.34%) than the TB scaffolds (8.01 ± 0.9%).

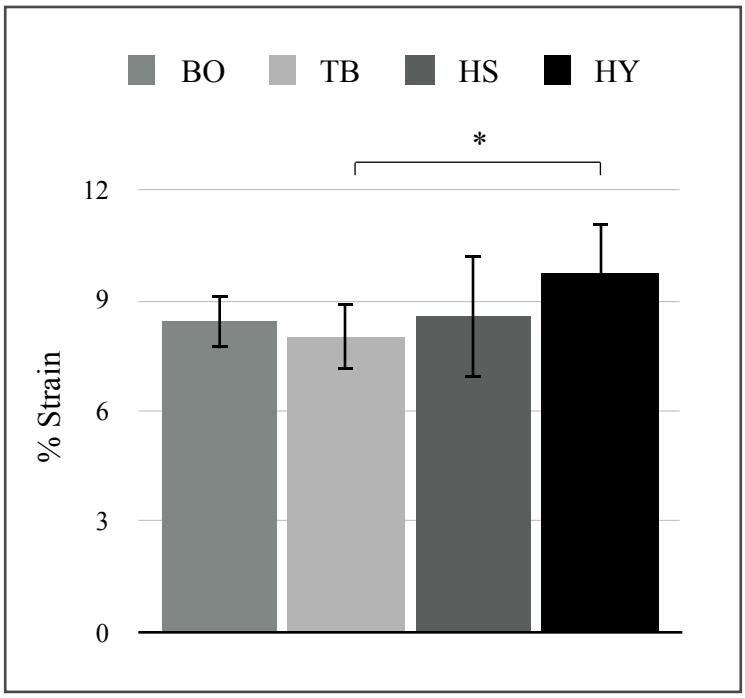

Figure 10: Toe region

The two scaffolds with the hydrogel-HS (64.64 ± 7.20%) and HY (72.46 ± 4.59%) exhibited significantly higher stains at failure than the TB (50.46 ± 5.30%) and the BO (49.00 ± 5.40%) scaffolds. The HY also displayed a significantly higher strain at failure than the HS scaffolds as shown in Figure 11 (a).

The BO scaffolds exhibited the highest elastic modulus at 425.79 ± 38.68 MPa. This is significantly higher that of the TB, HS and HY scaffolds which displayed moduli of 315.28 ± 18.81 MPa, 293.01 ± 43.43 MPa and 248.90 ± 15.47 MPa respectively. The TB and HS scaffolds also showed significantly higher moduli than the HY scaffolds.

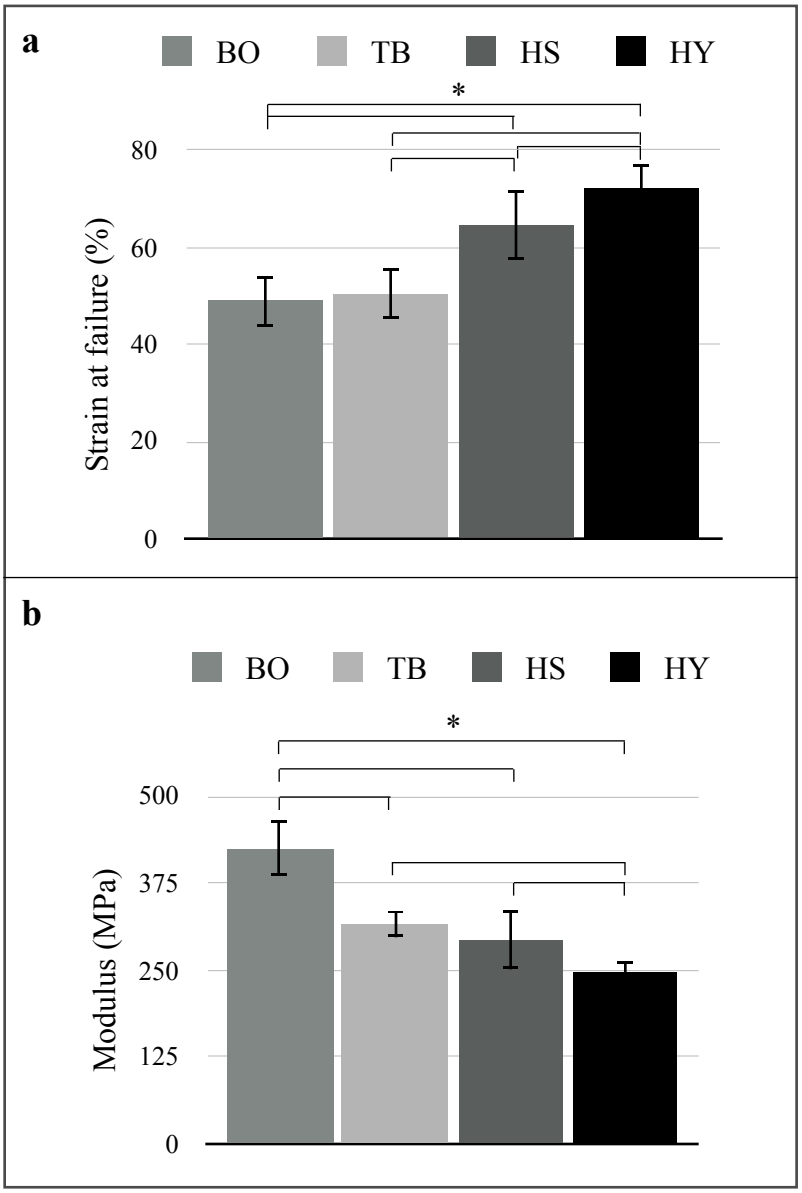

Figure 11: (a) Strain at failure (%) (b) Elastic modulus (MPa)

2.2.5 Fatigue Analysis

A significant decrease in the maximum load after 2000 cycles was observed for all but the twist-braid scaffolds. In case of maximum extension before failure, a significant difference was only observed in case of HY scaffolds.

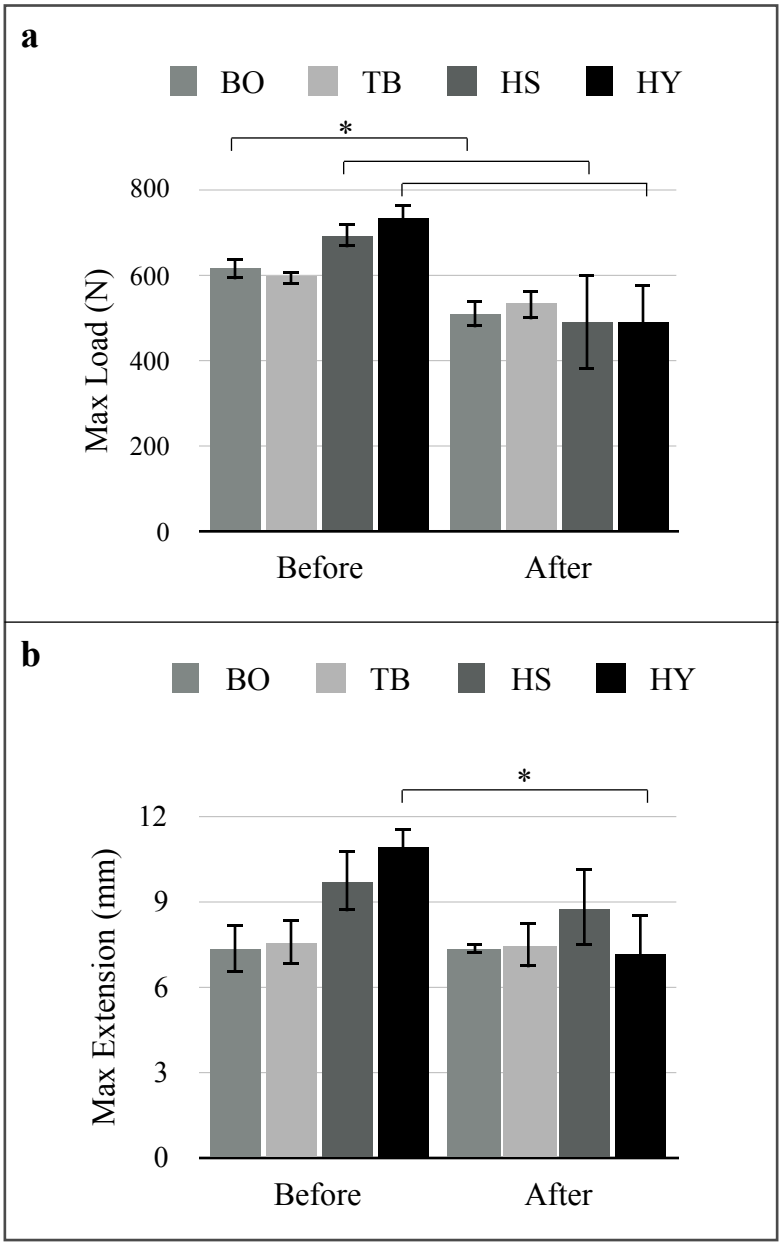

Figure 12: The trends observed in (a) Maximum load and (b) Maximum extension before and after applying cyclic strain (2000 cycles)

The ultimate tensile strength significantly decreased for all but the TB scaffolds. A significant drop in the strain at failure is observed only with HY scaffolds.

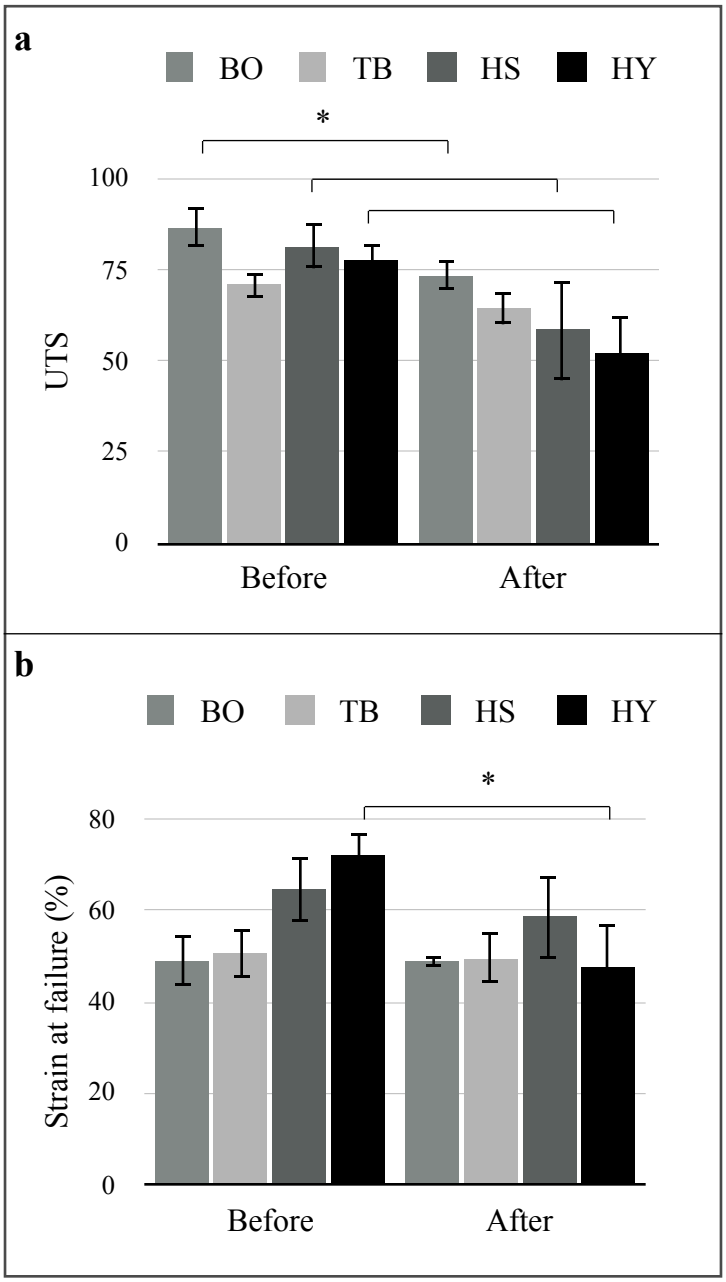

Figure 13: (a) Ultimate tensile stress, (b) Strain at failure

From Figure 14, it can be observed that elastic moduli of all four types of scaffolds decreased after subjecting them to 2000 cycles of strain but this drop was only significant in the BO and HS scaffolds.

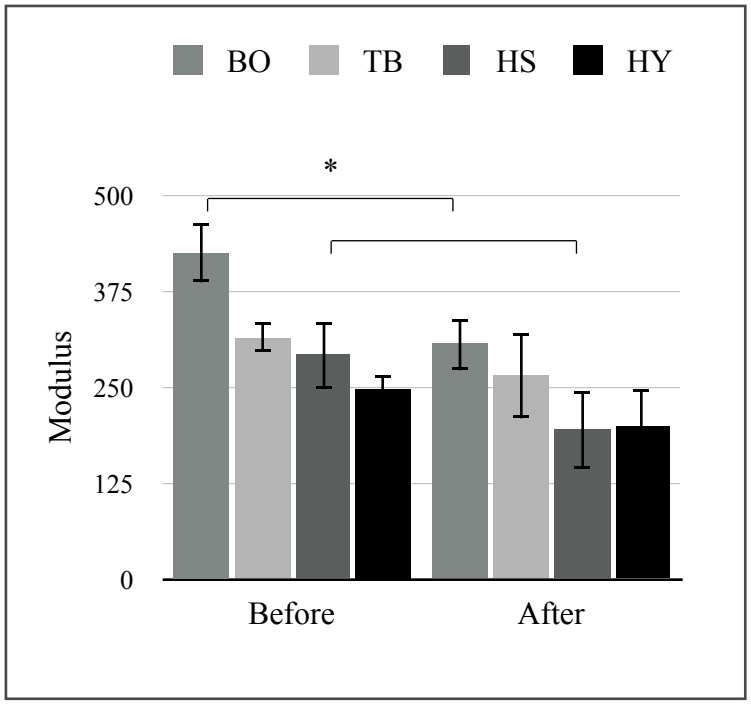

Figure 14: Elastic modulus

2.2.6 Cell Viability

The seeding efficiency calculated at Day 1 was approximately 95% for the BO scaffolds, 82% for the TB scaffolds, 80% for the HS scaffolds and 91% for the HY scaffolds.

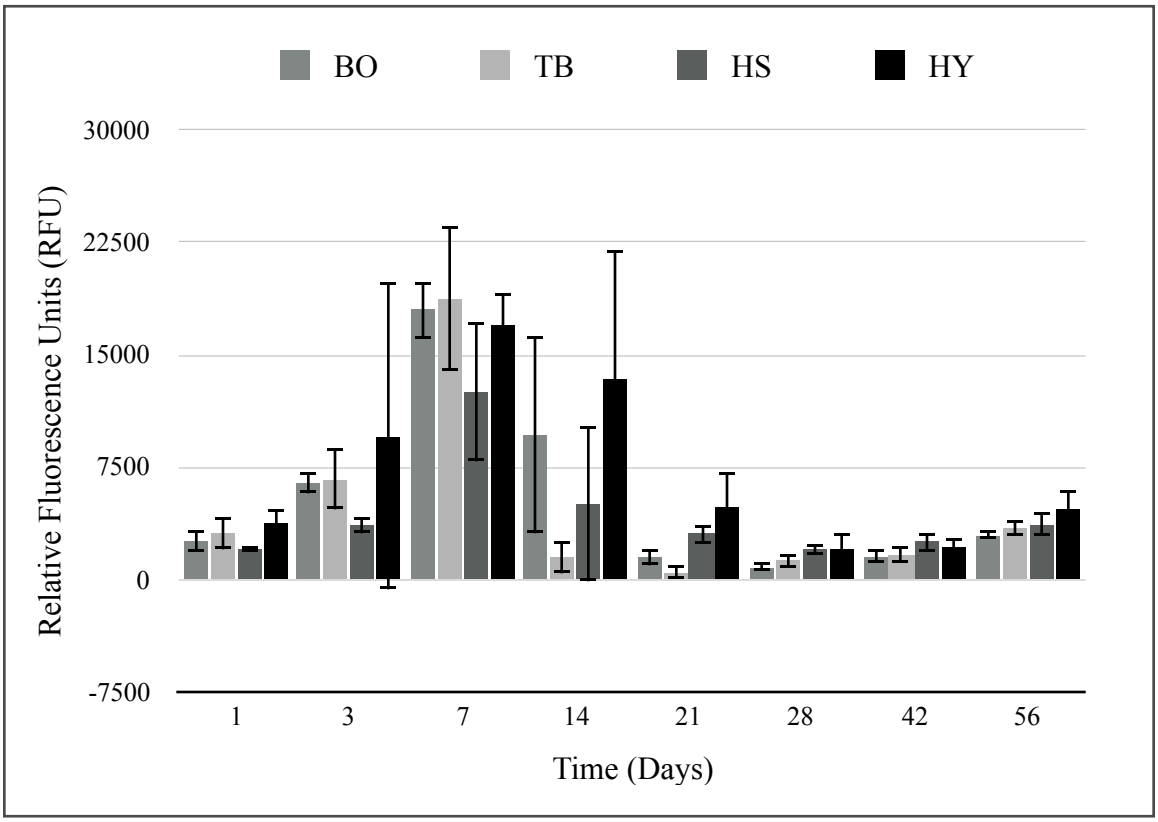

Figure 15: Cell viability data obtained over the course of the 8 week study (n=6).

The above graph shows the data obtained from the PrestoBlue assays that were performed at various time intervals. It can be observed that the cell viability increases steadily until day 7 following which a drop is seen at day 14. At day 21, a significant decrease in the viability is seen following which there are very small changes in the cell viability until 8 weeks.

2.2.7 Total Protein Estimation

The following graph shows the amount of protein released into the media at different time points as determined using the BCA assay. The data shows a significant increase in the amount of protein released into the media at day 14 for all the scaffolds.

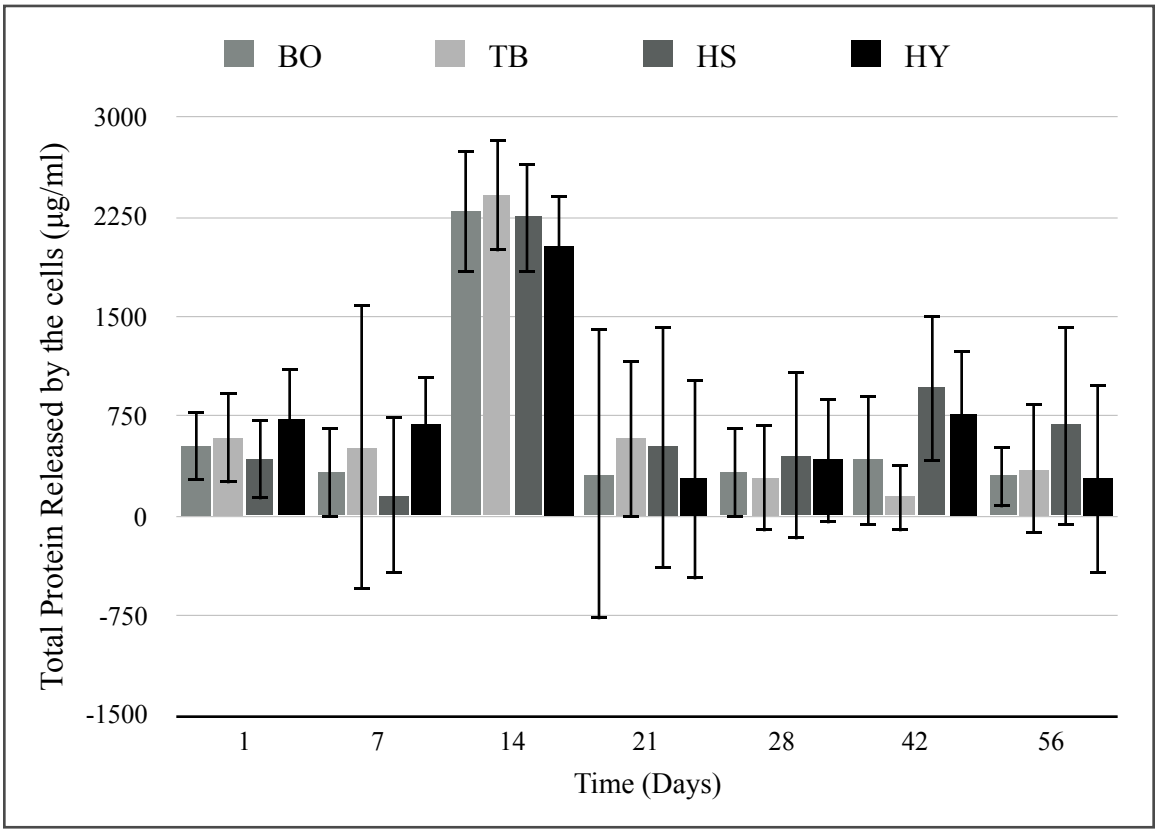

Figure 16: Data obtained from the BCA Assay over the course of the 8 week study (n=6)

2.2.8 Staining for Collagen

The scaffolds, 8 weeks after being seeded with cells looked as shown below when stained with picrosirius red.

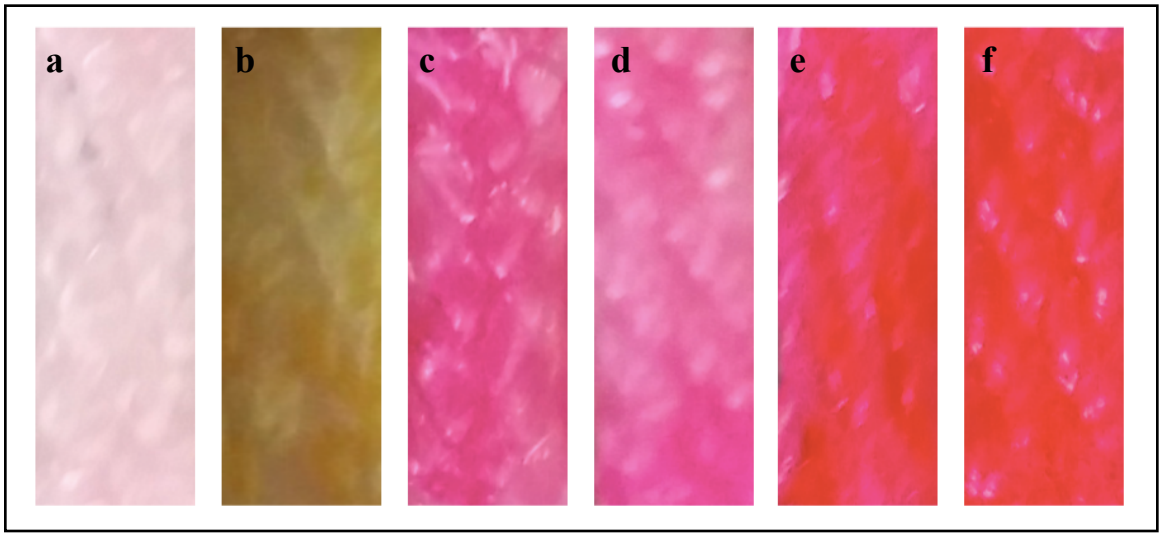

Figure 17: Scaffolds stained with picrosirius red. (a) Blank scaffold (no cells), (b) Blank Scaffold with PEGDA, (c) BO, (d) TB, (e) HS, (f) HY

In Figure 17, Scaffold (a) is a blank scaffold (no cells were seeded on it) that was stained. The absence of any color indicates that the scaffold itself did not get stained and the color observed in case of the other scaffolds is because of the collagen present. The reddish-pink color indicates the presence of collagen which is observed in case of all four types of scaffolds (c to f). Scaffold (b) is a blank scaffold with PEGDA (no cells were seeded on it but it contains hydrogel). The yellow-orange color seen with this scaffold indicates that the hydrogel retained some stain. The brighter color with the HS and HY can be attributed to this i.e. the hydrogel retaining stain. The following table (Table 1) shows the values of color intensity measured for the different scaffolds shown in Figure 17. The

scaffold images were converted to 8-bit images and the intensity values were analyzed using ImageJ (the maximum intensity is denoted by 0 and the minimum is 255 for 8-bit images).

Scaffold	Area	Mean	SD	Min	Max
Blank	41154	219.019	5.687	190	241
Blank with PEGDA	41154	110.897	13.769	79	158
BO	41154	143.426	17.722	98	211
TB	41154	164.971	16.017	122	220
HS	41154	108.713	15.638	72	197
HY	41154	102.556	14.255	78	194

Table 1: Intensity of color obtained for different scaffolds

The intensity value obtained for the Blank scaffold is 219.019 ± 5.687 which indicates that it had the lowest intensity. The TB and BO scaffolds exhibit intensities of 164.971 ± 16.017 and 143.426 ± 17.772 which are higher than those observed for the blank. The HS and HY scaffolds displayed the lowest values i.e. 108.713 ± 15.638 and 102.556 ± 14.255 which indicate that these showed the highest intensity.

2.2.9 Scanning Electron Microscopy Images

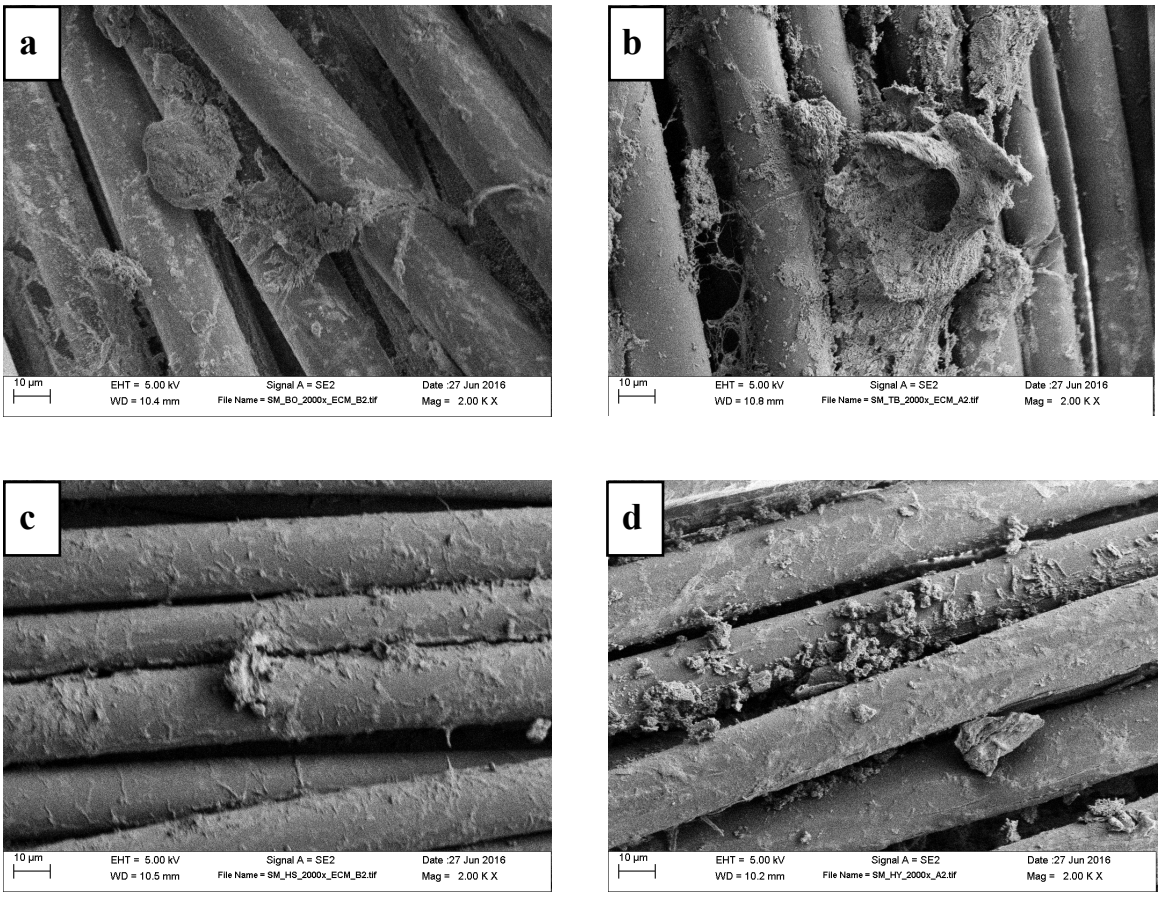

Figure 18: Scanning Electron Microscopy Images obtained after the 8 weeks cell study at 2000x showing extracellular matrix deposition (a) BO, (b) TB, (c) HS and (d) HY

Figure 18 shows the scanning electron microscopy images obtained for the four types scaffolds after 8 weeks of cell study. From these images, it can be observed that there was deposition of fibrous matrix on all of them i.e. the BO, TB, HS and HY scaffolds.

2.3 Discussion

This project involved the fabrication of two types of scaffolds-the braided only and the twist-braid scaffolds. Further, hydrogel PEGDA was incorporated into the TB scaffolds in two different ways. All the scaffolds were braided at a height of 31 cm.

The cross-sectional area data showed that TB, HS and HY scaffolds all had significantly larger cross-sectional areas than the BO scaffolds. It was also observed that the incorporation of hydrogel resulted in a significant increase in the area, with the HY scaffolds exhibiting the largest cross-sectional area. An increasing trend was also observed in terms of the weight per unit length (BO<TB<HS<HY). This observation that the HY scaffolds weighed more than the HS scaffolds, shows that significantly more hydrogel was incorporated in case of the HY scaffolds. It also indicates that despite braiding after the incorporation of the hydrogel onto the individual yarns, there wasn't a significant loss of hydrogel during the braiding process. The data obtained from liquid extrusion porosimetry showed that the median pore diameter was significantly higher for the BO scaffolds. The pore size distribution data showed that BO scaffolds had a higher percentage of larger pores when compared to the TB scaffolds.

The results from the mechanical tests show that both the braided-only and the twist-braid scaffolds (both with and without hydrogel) exhibit favorable mechanical properties. The data from the stress-relaxation tests showed that the normalized stress values obtained for all the scaffolds at 1000 seconds were comparable to the 70% obtained for the native ACL [45]. This data also showed that the incorporation of twisting lead to the twist-braid

scaffolds being significantly more viscoelastic than the braided-only scaffolds. Results from the tensile tests showed that the scaffolds with hydrogel i.e. the HS and HY can withstand significantly higher tensile loads. Hydrogels absorb water and release it when under stress. While the addition of twisting did make the scaffolds viscoelastic, hydrogel PEGDA was incorporated to more closely mimic the viscoelastic feature of ligaments. Incorporation of PEGDA lead to a larger toe region, increased load bearing capabilities and overall mechanical properties that were comparable to the native ACL. The TB and HS scaffolds showed significantly higher moduli than the HY scaffolds. This again shows that the incorporation of the hydrogel significantly reduced the stiffness of the scaffolds which would help prevent them from failure under high stress conditions. Following the application of cyclic strain, a significant decrease in maximum load was observed for the BO, HS and HY scaffolds. The ultimate tensile strength (UTS) also showed a significant decrease for all but the TB scaffolds, indicating that these scaffolds are able to withstand cyclic strain and are not as susceptible to fatigue as the rest of the scaffolds. After cyclic loading, the changes observed in mechanical properties of TB scaffolds were not significant, which could be a result of fiber twisting. Incorporation of fiber twisting allows the scaffolds to be strained to a greater extent without directly stretching out the individual PLLA fibers [19]. This is similar to the stretching out of the crimp pattern observed in native ligaments. Fiber twisting replicates the crimp pattern, improving strength and fatigue resistance of the scaffolds.

After the fatigue tests, a significant difference in maximum extension before failure of a scaffold was only observed in case of the HY scaffolds. This significant decrease can be attributed to the loss of hydrogel or the scrapping away of hydrogel due to the application of cyclic strain for an extended period of time. A significant drop in the strain at failure was also observed only with HY scaffolds. This can again be due to the loss of hydrogel during the process of cyclic strain.

Property	**Braided Only**	**Twist-Braid**	**Hydrogel Scaffold**	**Hydrogel Yarns**	**Native Human ACL [45]**
UTS (MPa)	86.379 ± 5.460	70.826 ± 3.402	81.592 ± 5.956	77.411 ± 4.366	37.8 ± 9.3
Toe region (% Strain)	8.417 ± 0.753	8.007 ± 0.909	8.535 ± 1.662	9.741 ± 1.344	2 - 4.8
Strain at failure (% Strain)	49.004 ± 5.402	50.460 ± 5.302	64.641 ± 7.204	72.460 ± 4.586	44.3 ± 8.5
Modulus (MPa)	425.790 ± 38.675	315.280 ± 18.808	293.014 ± 43.429	248.902 ± 15.472	111 ± 26

Table 2: Comparison of scaffold mechanical properties and the native human ACL

Table 2 shows that results obtained for all the scaffolds-BO, TB, HS and HY and a comparison to the mechanical properties of the native human ACL. It can be observed that all scaffolds have mechanical properties that are superior to the native human ACL.

This is essential to maintaining the mechanical properties throughout the polymer degradation process.

The results obtained from the PrestoBlue assay show that the cell viability increased steadily until day 7 for all the scaffolds, following which a drop was observed at day 14. This indicates that the cells were growing at a steady pace for the first 7 days. The drop at day 14 could be a result of the cells reaching confluence and starting to lay down extracellular matrix. The data obtained from the BCA assay showed a significant increase in the amount of protein released at day 14. This shows that the fibroblasts did indeed lay down extracellular matrix between days 7 and 14. At day 21, a significant decrease in the cell viability was seen following which there were very small changes in the cell viability until the end of 8 weeks. This decrease in viability shows that the cells may have gone into a state of quiescence after reaching confluence. There may have been some amount of cell death due to the cells not receiving sufficient nutrients. As the cell debris was washed away (through changing media), the remaining cells received nutrients bringing them out of their state of quiescence and leading to cell growth. This may be the cause of the small increase in cell viability that is observed from Day 28 to 8 weeks.

The images obtained after staining the scaffold with picrosirius red (after 8 weeks) showed that the HS and HY scaffolds exhibited higher color intensities. This was due to the retention of stain by the hydrogel PEGDA as shown with the blank scaffold containing PEDGA that was stained a yellow-orange color. The higher intensity of color

does not indicate that there was more collagen deposition with these scaffolds. From the intensity values shown in Table 1 and the images in Figure 17, it can be concluded that collagen was deposited on all four types of scaffolds. The scanning electron microscopy images in Figure 18 further confirm that there was deposition of extracellular matrix on all four types of scaffolds.

CHAPTER 3 - Conclusions and Future Directions

An ideal tissue engineered graft for ligament replacement has to be biocompatible, biodegradable and mimic the biomechanical properties of the native human ligament. PLLA was the material of choice because it biodegradable, approved by the FDA for various clinical applications and does not induce a permanent foreign body response [37]. PLLA also degrades over a longer period of time (>24 months) when compared to other polyhydroxyesters such as PGA (6 to 12 months) and PLGA (1 to 6 months) [27]. This is essential since the graft has to allow regeneration of new tissue while maintaining its mechanical properties.

In this study, the four different types if scaffolds i.e. the braided-only, the twist-braid and the two scaffolds with the hydrogel PEGDA were all found to mimic the mechanical properties of the native human ACL. After subjecting all the scaffolds to 2000 cycles of strain, only the twist-braid scaffolds showed changes in mechanical properties that were not significant. The TB scaffolds displayed resistance to fatigue, indicating that the incorporation of fiber-twisting can provide better long term mechanical stability.

Cell adhesion, proliferation and extracellular matrix deposition were observed with all the scaffolds, proving their biocompatibility. Future work would involve creating a steady supply of nutrients to the cells and the application of differentiation cues in order to study tissue integration and vascularization. The concentration of PEGDA will be varied and

different hydrogel phases will be evaluated to optimize the viscoelastic behavior of the TB scaffolds. Scanning electron microscopy can be used to obtain images through out the course of the cell study to study cell adhesion on different types of scaffolds as well as see if there any differences in how the cells proliferate on them. Further, in vivo studies will have to be performed to show if the implanted scaffolds can promote tissue regeneration and maintain mechanical stability.

REFERENCES

1. Chung, Eun Ji, et al. "A biodegradable tri−component graft for anterior cruciate ligament reconstruction." Journal of tissue engineering and regenerative medicine (2014).

2. Yates, E. W., et al. "Ligament tissue engineering and its potential role in anterior cruciate ligament reconstruction." Stem cells international 2012 (2011).

3. Bach, Jason S., et al. "Design considerations for a prosthetic anterior cruciate ligament." Journal of Medical Devices 6.4 (2012): 045004.

4. Laurencin, Cato T., and Joseph W. Freeman. "Ligament tissue engineering: an evolutionary materials science approach." Biomaterials 26.36 (2005): 7530-7536.

5. Wang, James H-C. "Mechanobiology of tendon." Journal of biomechanics 39.9 (2006): 1563-1582

6. Smith, Brian A., Glen A. Livesay, and S. L. Woo. "Biology and biomechanics of the anterior cruciate ligament." Clinics in sports medicine 12.4 (1993): 637-670.

7. Siegel, Leon, Carol Vandenakker-Albanese, and David Siegel. "Anterior cruciate ligament injuries: anatomy, physiology, biomechanics, and management." Clinical Journal of Sport Medicine 22.4 (2012): 349-355.

8. Giuliani, Jeffrey R., Kelly G. Kilcoyne, and J. P. Rue. "Anterior cruciate ligament anatomy: a review of the anteromedial and posterolateral bundles." The journal of knee surgery 22.2 (2009): 148-154.

9. Li, Guoan, et al. "In vivo elongation of the anterior cruciate ligament and posterior cruciate ligament during knee flexion." The American journal of sports medicine 32.6 (2004): 1415-1420.

10. Kakarlapudi, Trinath K., and Derek R. Bickerstaff. "Topic in Review: Knee instability: isolated and complex." Western Journal of Medicine 174.4 (2001): 266.

11. Freeman, Joseph W. "Tissue engineering options for ligament healing." Bone and Tissue Regeneration Insights 2 (2009): 13.

12. Laurencin, Cato T., and Yusuf Khan. "Regenerative engineering." Science translational medicine 4.160 (2012): 160ed9-160ed9.

13. Frank, C. B. "Ligament structure, physiology and function." Journal of Musculoskeletal and Neuronal Interactions 4.2 (2004): 199.

14. Walsh, William R., ed. Repair and regeneration of ligaments, tendons, and joint capsule. Springer Science & Business Media, 2007.

15. Freeman, Joseph W., et al. "Evaluation of a hydrogel–fiber composite for ACL tissue engineering." Journal of biomechanics 44.4 (2011): 694-699.

16. Kwansa, Albert L., et al. "Novel matrix based anterior cruciate ligament (ACL) regeneration." Soft Matter 6.20 (2010): 5016-5025.

17. Barber, John G., et al. "Braided nanofibrous scaffold for tendon and ligament tissue engineering." Tissue Engineering Part A 19.11-12 (2011): 1265-1274.

18. Liu, Yang, H. S. Ramanath, and Dong-An Wang. "Tendon tissue engineering using scaffold enhancing strategies." Trends in biotechnology 26.4 (2008): 201-209.

19. Freeman, Joseph W., Mia D. Woods, and Cato T. Laurencin. "Tissue engineering of the anterior cruciate ligament using a braid–twist scaffold design." Journal of biomechanics 40.9 (2007): 2029-2036.

20. Panariello, Robert A., Timothy J. Stump, and Dean Maddalone. "Postoperative Rehabilitation and Return to Play After Anterior Cruciate Ligament Reconstruction." Operative Techniques in Sports Medicine (2015).

21. Kramer, Lauren C. "Understanding and Preventing Noncontact ACL Injuries." Athletic Training and Sports Health Care 2.1 (2010): 43-44.

22. Yu, Bing, and William E. Garrett. "Mechanisms of non-contact ACL injuries." British journal of sports medicine 41.suppl 1 (2007): i47-i51.

23. Shirazi, Ali Negahi, et al. "Anterior cruciate ligament: structure, injuries and regenerative treatments." Engineering Mineralized and Load Bearing Tissues. Springer International Publishing, 2015. 161-186.

24. Ma, Jinjin, et al. "Three-dimensional engineered bone–ligament–bone constructs for anterior cruciate ligament replacement." Tissue Engineering Part A 18.1-2 (2011): 103-116.

25. Shelton, Walter R., and Bryan C. Fagan. "Autografts commonly used in anterior cruciate ligament reconstruction." Journal of the American Academy of Orthopaedic Surgeons 19.5 (2011): 259-264.

26. Agel, Julie, Elizabeth A. Arendt, and Boris Bershadsky. "Anterior cruciate ligament injury in National Collegiate Athletic Association basketball and soccer a 13-year review." The American journal of sports medicine 33.4 (2005): 524-531.

27. Petrigliano, Frank A., David R. McAllister, and Benjamin M. Wu. "Tissue engineering for anterior cruciate ligament reconstruction: a review of current strategies." Arthroscopy: The Journal of Arthroscopic & Related Surgery 22.4 (2006): 441-451.

28. Chen, Chih-Hwa, Wen-Jer Chen, and Chun-Hsiung Shih. "Arthroscopic anterior cruciate ligament reconstruction with quadriceps tendon-patellar bone autograft." Journal of Trauma and Acute Care Surgery 46.4 (1999): 678-682.

29. Cooper, James A., et al. "Evaluation of the anterior cruciate ligament, medial collateral ligament, achilles tendon and patellar tendon as cell sources for tissue-engineered ligament." Biomaterials 27.13 (2006): 2747-2754.

30. Legnani, Claudio, et al. "Anterior cruciate ligament reconstruction with synthetic grafts. A review of literature." International orthopaedics 34.4 (2010): 465-471.

31. Altman, Gregory H., et al. "Silk matrix for tissue engineered anterior cruciate ligaments." Biomaterials 23.20 (2002): 4131-4141.

32. Cooper, James A., et al. "Fiber-based tissue-engineered scaffold for ligament replacement: design considerations and in vitro evaluation." Biomaterials 26.13 (2005): 1523-1532.

33. Fu, Freddie H., et al. "Current trends in anterior cruciate ligament reconstruction part 1: biology and biomechanics of reconstruction." The American Journal of Sports Medicine 27.6 (1999): 821-830.

34. Beasley, Leslie S., et al. "Anterior cruciate ligament reconstruction: a literature review of the anatomy, biomechanics, surgical considerations, and clinical outcomes." Operative Techniques in Orthopaedics 15.1 (2005): 5-19.

35. Dunn, Michael G., et al. "Development of fibroblast−seeded ligament analogs for ACL reconstruction." Journal of biomedical materials research 29.11 (1995): 1363-1371.

36. Ge, Zigang, et al. "Biomaterials and scaffolds for ligament tissue engineering." Journal of Biomedical Materials Research Part A 77.3 (2006): 639-652.

37. Lu, Helen H., et al. "Anterior cruciate ligament regeneration using braided biodegradable scaffolds: in vitro optimization studies." Biomaterials 26.23 (2005): 4805-4816.

38. Leong, Natalie Luanne, et al. "Evaluation of polycaprolactone scaffold with basic fibroblast growth factor and fibroblasts in an athymic rat model for anterior cruciate ligament reconstruction." Tissue Engineering Part A 21.11-12 (2015): 1859-1868.

39. Mooney, David J., and Joseph P. Vacanti. "Tissue engineering using cells and synthetic polymers." Transplantation Reviews 7.3 (1993): 153-162.

40. Vacanti, J. P. "Tissue engineering and the road to whole organs." British Journal of Surgery 99.4 (2012): 451-453.

41. Silver, F. H., et al. "Anterior cruciate ligament replacement: a review." Journal of long-term effects of medical implants 1.2 (1990): 135-154.

42. Butler, David L., et al. "Location-dependent variations in the material properties of the anterior cruciate ligament." Journal of biomechanics 25.5 (1992): 511-518.

43. Cooper, James A., et al. "Biomimetic tissue-engineered anterior cruciate ligament replacement." Proceedings of the National Academy of Sciences 104.9 (2007): 3049-3054.

44. Pioletti, Dominique P., and Lalao R. Rakotomanana. "On the independence of time and strain effects in the stress relaxation of ligaments and tendons." Journal of biomechanics 33.12 (2000): 1729-1732.

45. Noyes, Frank R., and Edward S. Grood. "The strength of the anterior cruciate ligament in humans and Rhesus monkeys." J Bone Joint Surg Am 58.8 (1976): 1074-1082.